PAPER • **OPEN ACCESS**

On the fabrication and mechanical modelling microscale bistable tensegrity systems

To cite this article: Z Vangelatos *et al* 2020 *IOP Conf. Ser.: Mater. Sci. Eng.* **999** 012002

IOP Conf. Series: Materials Science and Engineering **999** (2020) 012002 doi:10.1088/1757-899X/999/1/012002

On the fabrication and mechanical modelling microscale bistable tensegrity systems

Z Vangelatos[1], I Farina[2] A Micheletti[3], N Singh[4], C P Grigoropoulos[1], F Fraternali[4]

[1] Department of Mechanical Engineering, University of California, Berkeley, CA, USA.
[2] Department of Engineering, University of Naples Parthenope, Italy
[3] Department of Civil and Computer Science Engineering, University of Rome Tor Vergata, Italy
[4] Department of Civil Engineering, University of Salerno, Italy
Email: zacharias_vangelatos@berkeley.edu; micheletti@ing.uniroma2.it; snarinder@unisa.it; cgrigoro@berkeley.edu; f.fraternali@unisa.it

Abstract. We report about the analysis, design, and experimental testing of modular structures composed of bistable units derived from the classic triangular tensegrity prism. Tensegrity structures are pin-connected frameworks, composed by bars and cables, possessing internal mechanisms and self-stress states, and featuring a variety of structural responses depending on their prestress, edge connectivity, and geometry. When a tensegrity system has only one internal mechanism and one self-stress state, as in the triangular prism case, it is possible to associate to it a corresponding bistable unit, by replacing all cables with bars and changing their edge-lengths slightly. After presenting experimental results of compression tests carried out on microscale specimens fabricated through multiphoton lithography, we compare them with the numerical predictions obtained by our computational model.

1. Introduction

In recent times, architected metamaterials, structural systems whose physical behavior depends on the way they are designed rather than from the bulk properties of the constituent material, are attracting more and more attention from the scientific community. Metamaterials are designed to obtain extraordinary mechanical properties, such as exceptional strength-to-weight and stiffness-to-weight ratios, frequency bandgaps, negative overall elastic moduli, negative mass density, auxeticity, and solitary wave propagation [1]-[13]. Bistability is one of the difficult-to-find and most desired features in current studies on architected materials [14]-[19]. Further, tensegrity systems, pin-connected prestressed frameworks composed by bars and cables, constitute a particular structural class in that their response to statical and dynamical actions include a rich variety of non-linear effects [20][21][10]-[13]. We here focus on the Bistability property of some tensegrity structures [21] to design and fabricate bistable latticed structures at the nanoscale with the help of unique multiphoton lithography [23].

2. Bistable lattices with tensegrity architecture

Tensegrity systems are characterized by the existence of a self-stress state, and they can also possess internal mechanisms, which are nodal displacements which cause null first- order elongation of the elements, excluding rigid-body displacements. Self-stress states and mechanisms belongs to the left

and right null spaces of the equilibrium operator, expresses the linear relationship between the axial forces in the elements and the external loads [24].

We consider here the subclass of tensegrity systems possessing a single internal mechanism and a single self-stress state, which means that the equilibrium operator is represented by a rank- deficient square matrix, with rank deficiency equal to one. Stable tensegrity systems with internal mechanisms satisfy the so-called prestress-stability condition, signifying that the self- stress state imparts first-order geometric stiffness to any internal mechanism, which are then referred to as first-order infinitesimal mechanisms [24].

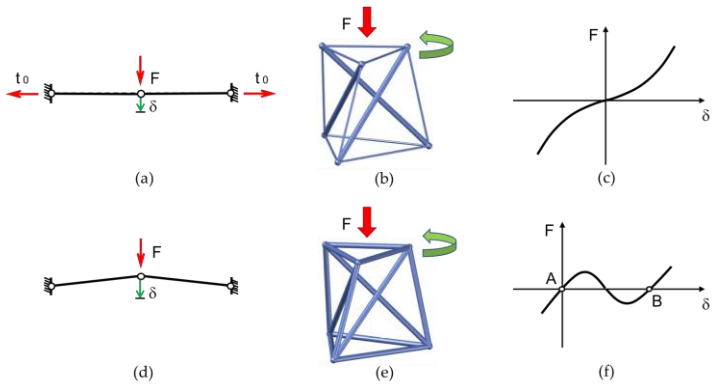

Figure 1. (a) Three-aligned-hinges system. (b) Triangular tensegrity prism. (c) Monostable load-vs-displacement plot. (d) Simple bistable system. (e) A bistable bar-framework corresponding to the tensegrity prism in (b). (f) Bistable load-vs-displacement plot. Curved green arrows in (b) and (e) indicate the twisting of the top base in the relative screw motion between bases.

Figure 1 illustrates the behavior of two prestress-stable systems, the simple three-aligned-hinges system Fig.1(a) [25], and the classical tensegrity prism (Fig. 1, b), when they are subjected to a load activating the mechanism. The typical load-vs-displacement curve is of stiffening type, and it can be approximated by a cubic with an inflexion point at the origin (Fig. 1, c). The slope at the origin is directly proportional to the level of self-stress t_0 in the elements. It can be verified that, by reversing the sign of prestress of a tensegrity system with the above-mentioned properties, the equilibrium configuration becomes unstable, and that two other stress-free stable equilibrium configurations arise (Fig. 1, d, e). The response to a load activating the internal mechanism is then of bistable type (Fig. 1, f) and it is associated to a double-well elastic energy. In the stable prestressed equilibrium configuration (triangular tensegrity prism), the top base is rotated with respect to the bottom base by an angle equal to $\theta_0 = \pi/6$, which is referred to as the *twist angle at equilibrium* (*c*f [20]). This value does not change when considering different circumscribed radii of the two bases, as shown in Fig.1(b). The first-order infinitesimal mechanisms are a relative screw motion (roto-translation) between bases, with the screw axis passing through the bases' centroids. The corresponding bistable unit is obtained by replacing cables with bars, and realizing the edge-lengths so as to have a twist angle slightly different from $\pi/6$. The structure is stress-free in this configuration, which we name as *primary stable configuration* (corresponding to point A in Fig. 1, f). When applying a vertical load to the top base, while having the bottom base fixed to the ground, the system snaps into the *secondary stable configuration* (corresponding to point B in Fig.1(f), through a relative screw motion between bases, analogous to the mechanism of the original tensegrity structure.

3. Fabrication by MPL and indentation experiments

We designed the modular assembly for experimentation as shown in Fig. 2, where three double units are assembled together side by side, a double unit being composed of two prisms

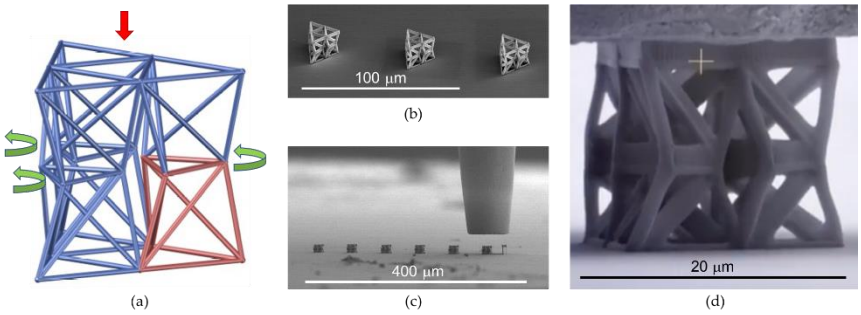

Figure 2. (a) Bistable assembly composed of six tensegrity prisms (one highlighted in red). (b, c) Fabricated samples. (d) View of a sample during the indentation experiment.

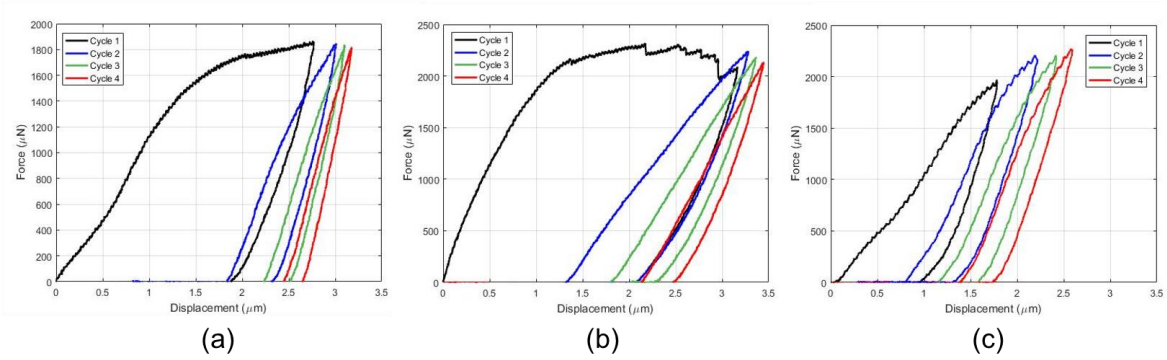

Figure 3. Force-vs-displacements plots for repeated loading-unloading cycles.

which is the mirror image of each other. The material for the specimens has been prepared by mixing organic-inorganic constituents in particular ratio as reported in ref. [22], such as: Zr-DMAEMA composed of zirconium prop oxide, (2-dimethylaminoethyl) methacrylate (DMAEMA) and ASTM type II deionized distilled water. After placing the mixture on a glass substrate in vacuum for 24 hours, specimen fabrication has been performed. Further details on the fabrication procedure are reported in [22]. The Young modulus of the fabricated material has been estimated with preliminary tests to be equal to E = 1.281 GPa. Indentation experiment have been performed by applying unilateral displacement-controlled loading-unloading cycles of increasing amplitude Fig. 2(c). Results of the testing are shown in Fig. 3. There is a marked softening behavior; the softening part of the curve leads to a secondary stable equilibrium configuration upon unloading; the secondary configuration is preserved during successive loading-unloading cycles; the curve presents a slight viscoelastic character. Moreover, it can be observed that, in association with the softening behavior, the three middle triangles undergo a twisting motion. In addition, the curves show that when the loads are close to the peak value, there can be microcracking events taking place termed as a sawtooth pattern in the curve.

4. Numerical experiments

We implemented a reduced-order model in a large-displacement regime based on the Stick &Spring approach (see, e.g. [26]-[28]). In the model, the nodal displacements are taken as Lagrangian parameters, while members can only extend or contract in a linearly elastic fashion, with stiffness constant ka, while they are rigid with respect to bending, shear, and torsion deformations. Additionally, the angular linearly elastic springs are placed at the nodes, with stiffness constant ks, to respond to changes in angle between the axes of pairs of members

which are not the part of a triangle.

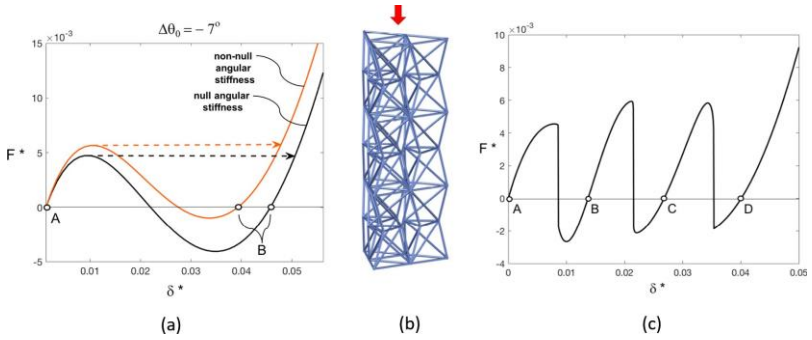

Figure 4. (a) Dimensionless force-vs-displacement plot obtained numerically for the bistable assembly, (b) Three-layer assembly. (c) Dimensionless force-vs-displacement plot of the three- layer assembly

Figure 4 shows the static response to a vertical downward load applied to the studied assembly. In the plot, the dimensionless load F^* is one third of the actual load divided by the stiffness constant of the shortest beam and by the beams' minimum diameter, while the dimensionless displacement δ is the vertical displacement divided by the height of the assembly. As to the geometric parameters in this simulation, we have that a/b = 0.7, a/h = 0.25, $\Delta\theta_0$ = 7degrees, where a and b are the circumscribed radii to the bottom and top bases of the unit, h is the height of the assembly, and $\Delta\theta_0 = \theta_0\ \pi/6$. The two curves differ in the value of the angular stiffness constant, this is null for the black curve, and it satisfies $k_s/(a^2k_a)$ = 0.00025 for the color (grey) curve. The simulation is consistent with the fact that in a force-controlled loading-unloading experiment, the system would snap from a primary stable configuration (corresponding to point A in Fig. 4 (a)) to a secondary stable configuration (corresponding to points B in Fig. 4(a)), passing along a softening-type path before snapping. A behavior which is qualitatively similar to that observed in the indentation experiments, while the differences can be partly ascribed to the viscoelastic behavior of the photo resistive material. We then performed the same numerical experiment on a three-layer assembly obtained by superposing copies of the previously considered system on top of each other (Fig. 4, b). The three layers differ from one another in the stiffness of the angular springs, which are chosen with a 5 percent difference from one layer to another in order to obtain a sequential snapping of the layers. Geometric parameters are the same as in the previous assembly, and $k_s/(a^2k_a)$ = 0.00021 for the middle layer. The resulting force-vs-displacement curve (Fig. 4, c) shows that there are multiple stable configurations (points A, B, C, D in Fig. 4, c), related to the bistable behavior of the individual layers.

5. Conclusions

In this research work, a bistable assembly composed of triangular tensegrity prisms has been designed, fabricated by MPL, and subjected to indentation testing.

The experimental force-vs-displacement curves highlight a softening response which brings the structure to a secondary stable equilibrium configuration. Such secondary configuration is maintained during successive loading-unloading cycles. In addition, a slight viscoelastic behavior is observed, together with occasional microcracking events.

A Stick & Spring reduced-order model is employed to simulate indentation experiment, confirming that the observed experimental behavior results from the bistable design of the constituent units.

A three-layer system is analyzed numerically to show that multi-stable lattices can be obtained.

Acknowledgements

This research is partially supported by the National Science Foundation (NSF) under the Scalable 475 Nanomanufacturing (SNM) Program, grant number 1449305. A.M. acknowledges financial support

from the Italian Ministry of Education, University, and Research (MIUR) under the PRIN 2017 National Grant '3D printing: a bridge to the future' (grant number 2017L7X3CS 004). N.S. and F.F. acknowledge financial support from MIUR under the PRIN 2017 National Grant 'Multiscale Innovative Materials and Structures' (grant number 2017J4EAYB).

References

[1] Liu Z, Zhang X, Mao Y, Zhu Y Y, Yang Z, Chan, C T and Sheng P 2000 *Science* **289** 1734–1736.
[2] Lu M H, Feng L and Chen Y F 2009 *Material Today* **12** pp 34-42.
[3] Maldovan M 2013 *Nature* **503** pp 209-217.
[4] Brunet T, Leng J and Mondain-Monva O 2013 *Science* **342** pp 323-324.
[5] Deng B, Mo C, Tournat V, Bertoldi K and Raney J R 2019 Physics Review Letter **123** pp 024101.
[6] Yildiz M E, Tran C A, Barchiesi E, Spagnuolo M, dell'Isola F and Hild F 2019 *State of the Art and Future Trends in Material Modeling* **100** p 485-505
[7] Meza L R, Das S and Greer J R 2014 *Science* **345** pp 1322–1326.
[8] Zheng X et al, 2014 *Science* **344** pp 6190.
[9] Phani A S, Hussein M I (eds) 2017 *Dynamics of Lattice Materials*, John Wiley & Sons, Ltd, Chichester, UK.
[10] Fraternali F, Senatore L and Daraio C 2012 *Journal of the Mechanics and Physics of Solids* **60** pp 1137-1144.
[11] Fraternali F, Carpentieri G, Amendola A, Skelton R E and Nesterenko V F 2014 *Applied Physics Letters* **105** pp 201903.
[12] Davini C, Micheletti A and Podio-Guidugli P 2016 *Meccanica* **51** pp 2763-2776.
[13] Micheletti A, Ruscica G and Fraternali F 2019 *Nonlinear Dynamics* **98** pp 2737-2753.
[14] Shan S, Kang SH, Raney J R, Wang P, Fang L, Candido F, Lewis J A and Bertoldi K 2015 *Advance Materials* **27** pp 4296-4301.
[15] Raney J R, Nadkarni N, Daraio C, Kochmann D M, Lewis J A and Bertoldi K 2016 *PNAS* **113** pp 9722-9727.
[16] Osama R B, Andr ́e F and Chiara D 2017 *Proceedings of the National Academy of Sciences* **114** pp 4603-4606.
[17] Chen T., Bilal O R, Shea K and Daraio C 2018 *Proceedings of the National Academy of Sciences* **115** 5698- 5702.
[18] Deng B, Wang P, Tournat V and Bertoldi K 2019 *Journal of the Mechanics and Physics of Solids* pp 103661
[19] Jeong H Y, An S, Seo I C 2019 *Sci Rep* 9324.
[20] Oppenheim I J and Williams W O 2000 *Journal. Elasticity* **59,** pp. 51–65.
[21] Micheletti A. 2013 *Proceedings of Royal Society* A 469.
[22] Vangelatos Z, Micheletti A, P Grigoropoulos C and Fraternali F. 2020 *Nanomaterials* **10(4)** pp 652.
[23] Sakellari I, Kabouraki E, Gray D, Purlys V, Fotakis C, Pikulin A, Bityurin N, Vamvakaki M and Farsari M 2012 *ACS Nano* 6:2302-2311.
[24] Calladine C R and Pellegrino S 1991 *International Journal of Solid Structure* **27** pp 505-515.
[25] C R Calladine 1978 *International Journal of Solids and Structures* **14** pp 161-172.
[26] Favata A, Micheletti A and Podio-Guidugli P 2014 *International Journal of Engineering Sciences* **80** pp 4-20.
[27] Amendola A, Favata A and Micheletti A 2018 *Frontiers in Materials* **5** pp 1-22.
[28] Favata A, Micheletti A, Podio-Guidugli P and Pugno N M 2017 *Meccanica* **52** pp 1601-1624.